Polydomain–Monodomain Orientational Process in Smectic-C Main-Chain Liquid-Crystalline Elastomers[a]

Antoni Sánchez-Ferrer,* Heino Finkelmann

The polydomain–monodomain (PM) transformation takes place when a polydomain of a smectic-C main-chain liquid-crystalline elastomer (SmC MCLCE) is uniaxially stretched. We present results based on a combination of mechanical and X-ray experiments which show how the domains initially rearrange to finally form a perfect conical layer distribution (monodomain) when the sample is fully stretched. The rearrangement and orientational process of the domains is quantified and compared to the parallel and perpendicular uniaxial stress–strain deformations of a monodomain sample. The stress–strain behaviour of the polydomain lays between the uniaxial deformations, parallel and perpendicular to the director, of the monodomain sample.

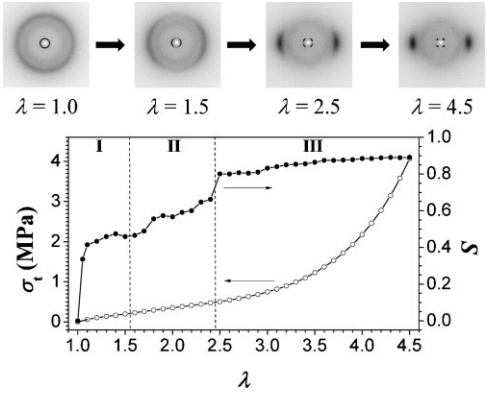

Introduction

Smectic main-chain liquid-crystalline elastomers (MCLCEs) exhibit different mechanical responses with respect to nematic elastomers, due to their layered structure. This effect is caused by distinct anisotropic mechanical properties under deformation processes – parallel or perpendicular to the smectic layer normal – when a force is applied on a conical layer distribution (monodomain).[1] Besides the differences in the mechanical response, orientational processes from polydomain-to-monodomain (PM) are of interest for the understanding of the formation of anisotropic systems.

First experiments on the characterisation of PM transitions were done on smectic-C (SmC) side-chain liquid-crystalline elastomers (SCLCEs) by stress–strain deformations combined with X-ray experiments[2] or by light scattering studies.[3] The first attempts to study PM transitions in main-chain systems were done on the frame of Smectic-A (SmA) main-chain liquid-crystalline thermosets,[4,5] where four distinct regions were found from stress–strain deformations and stress relaxation experiments:[6] a linear viscoelastic deformation, a homogeneous yielding, a strain softening and a strain hardening region. The first experiment on main-chain networks was done on SmA and nematic MCLCEs,[7] and dynamic mechanical analysis already showed differences with respect to side-chain systems.

Since smectic materials show shape memory effect,[8] some experiments were done in order to obtain monodomain samples (conical layer distribution) by stretching the initial polydomain.[9] Mechanical experiments on those systems

A. Sánchez-Ferrer
Food & Soft Materials Science Group, Institute of Food, Nutrition & Health, ETH Zurich, Schmelzbergstrasse 9, 8092 Zurich, Switzerland
Fax: +41 44 632 1603; E-mail: antoni.sanchez@agrl.ethz.ch
A. Sánchez-Ferrer, H. Finkelmann
Albert Ludwigs University, Institute for Macromolecular Chemistry, Stefan-Meier-Str. 31, 79104 Freiburg, Germany

[a] Supporting information for this article is available at the bottom of the article's abstract page, which can be accessed from the journal's homepage at http://www.mrc-journal.de, or from the author.

DOI: 10.1002/marc.201000590

showed the presence of three regions: an elastic deformation, neck propagation and deformation of the necked monodomains.[10] Other studies showed the mechanical behaviour of SmC MCLCEs as function of the crosslinking density, where the necking effect appeared at high degrees of crosslinking, while a soft plateau region was observed for low crosslinked elastomers.[11,12] Recently, the PM transition in a smectic-C_A (SmC_A) MCLCE was attributed to the change in the polymer backbone conformation from hairpinned to fully extended.[13]

SmC liquid-crystalline elastomers are also important as models for the understanding of SmC^* elastomers.[14] The chiral mesogens in MCLCEs are of significance because of their optical and ferroelectric properties when a pure monodomain – mesogens and layers are oriented – is obtained.[15,16] Theoretical models based on PM transitions were developed for nematic systems with local director rotations without change in the domains during the stress–strain plateau region,[17,18] and these models are supposed to also hold for smectic systems.[19] Other theoretical models have been developed for deformations in smectics,[20–24] and in more detail for SmA[25–28] and SmC[29–31] liquid-crystalline elastomers, but there is a lack of information from the experimental point of view.

In this paper, the mechanical response of a polydomain SmC MCLCE will be described under uniaxial deformation, and compared to its corresponding sample with conical layer distribution.[1] The PM transformation process of SmC MCLCE is studied in detail to identify the orientational mechanism, the rearrangement of the random distributed domains to a conical layer distribution formation, and the coupling with the applied external mechanical field.

Experimental Part

X-ray Diffraction Experiments

X-ray scattering experiments were performed using a Philips PW 1730 rotating anode (4 kW) in order to obtain direct information on the SAXS and WAXS reflections in the smectic-C phases. Cu K_α radiation (1.5418 Å) filtered by a graphite monochromator and collimated by a 0.8 mm collimator was used. The incident beam was normal to the surface of the film. The scattered X-ray intensity was detected by a Schneider image plate system (700 × 700 pixels, 250 μm resolution). Sample was placed in a self-constructed holder where temperature was controlled by a Haake-F3 thermostat. From the SAXS intensities the layer distance (d) and the correlation length (ξ), and the layer angle (ϕ) were calculated from a Gaussian distribution. From the WAXS intensities, the mesogen distance, and the mesogen angle (φ) from a Gaussian distribution, and the order parameter ($S = S_d \cdot S_N$) according to Lovell and Mitchell,[32,33] where S_d is the director order parameter and S_N the order parameter that refers to the local orientational order parameter. For samples having a macroscopically uniform alignment of the director we assume that $S_d \approx 1$. All error bars are calculated as a half of the FWHM from the intensity Gaussian distribution of the φ and ϕ.

Uniaxial X-ray Diffraction Experiments

Uniaxial deformations were carried out using a uniaxial stress–strain self-constructed apparatus. All measurements were done at 25 °C and 1 h of relaxation time after each stretching step.

Uniaxial Stress–Strain Experiments

Stress–strain measurements were performed with a self-constructed apparatus. In a cell controlled by a Haake-F6 thermostat and equipped with a Pt100 thermoresistor, the sample was stretched by one Owis SM400 microstep motor and controlled by an Owis SMK01 microstep controller. The stress (σ) was measured by a HBM PW4FC3 transducer load cell (300 g) and analysed by an HBM KW3073 high-performance strain gauge indicator. All relevant data such as temperature, uniaxial strain ($\lambda = L/L_0$) and uniaxial stress (σ) were continuously logged. A personal computer controlled the deformation stepwise as specified by a script file. After each deformation step, the static responses to the deformation, the uniaxial stress (σ) was recorded once equilibrium was reached according to the slope and the standard deviation of the continuously logged data.

Synthesis of the Polydomain of SmC MCLCE

The synthetic route for the obtaining of a polydomain of the SmC MCLCE is similar to the synthesis of monodomain samples, with minor changes. No load was applied to a piece of the partially crosslinked elastomer, in order to keep a polydomain sample, which contains randomly oriented microdomains of nanometer size. The crosslinking reaction was completed by leaving the elastomer in the oven under vacuum at 60 °C for 2 d. In order to measure the soluble content (5.7%) of the samples, the elastomer was placed in a liquid–solid extractor for 1 d, using hexane as solvent. All synthetic and characterisation details can be found in the literature, as well as the structures of the chemicals used for the synthesis of the SmC MCLCES (Scheme 1).[1,34,35]

Results and Discussion

Mechanical Properties of a Polydomain

The purpose of this study was to define how a polydomain of MCLCE responds differently with respect to the corresponding monodomain on applying an external mechanical field, and how this force couples to the director and/or to the layer orientation. In previous communications,[1,35] parallel and perpendicular deformations were applied to a monodomain of SmC MCLCE, showing a great difference between both uniaxial stretchings, but coupling between the applied mechanical field and the director, as

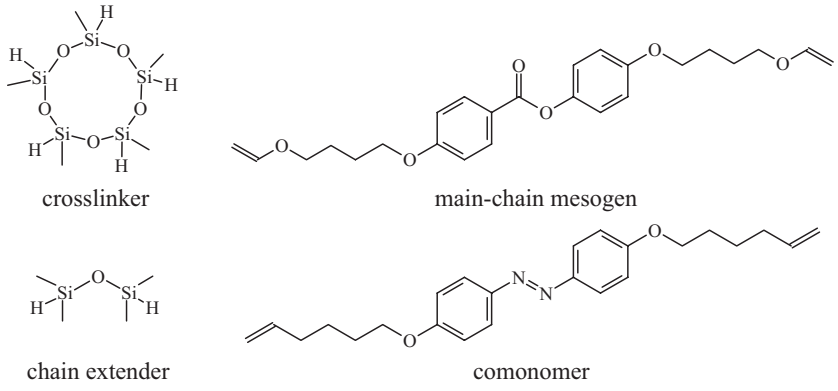

Scheme 1. Chemical structures of the compounds used for the synthesis of the SmC MCLCE.

well as between the field and the layers, was always observed.

A sample of a polydomain of SmC MCLCE was uniaxially stretched and compared with the deformation of its corresponding monodomain – parallel and perpendicular deformations with respect to the director. The corresponding monodomain had a conical distribution of the smectic layers. A perfect monodomain (mesogens and layers present at the same time) can only be achieved by further shear experiments.[1] Figure 1a shows the uniaxial stress–strain experiments for all three deformations on a polydomain and its corresponding monodomain. The results clearly show that the deformation of a polydomain is softer than the deformation parallel to the director of a monodomain, but a little bit harder than the perpendicular deformation to the director of the monodomain.

In order to reinforce in more detail this result, all three samples were evaluated following the expression for the description of the increase of true stress as function of the applied strain in smectic elastomers under uniaxial deformations (see Supporting Information, Figure SI-1, SI-2 and SI-3).[34]

$$\sigma_t(\lambda) = \sigma_{lin} + \sigma_{exp} + \sigma_{pre} = a(\lambda - 1) + b\left(e^{c(\lambda-1)} - 1\right) + d\left(1 - e^{-f(\lambda-1)}\right) \quad (1)$$

The fitting parameter 'a' corresponds to the linear behaviour of Young's modulus, 'b' and 'c' are the fitting parameters of the exponential growth.[36] The parameters 'd' and 'f' are the fitting parameters of the pre-stress region that are applied because of an extra energetic factor due to the presence of smectic layering. In these smectic systems, the enthalpy elasticity factor from the smectic layers plays an important role.[37–39]

The Young's modulus (slope) is calculated from the derivative of Equation 1 giving the following expression:

$$E(\lambda) = \frac{\partial \sigma_t}{\partial \lambda} = E_{lin} + E_{exp} + E_{pre} = a + b \cdot c \cdot e^{c(\lambda-1)} + d \cdot f \cdot e^{-f(\lambda-1)} \quad (2)$$

The polydomain deformation has a Young's modulus of $E = 0.56$ MPa (Table 1), which is closer to the value for the perpendicular deformation of the monodomain ($E = 0.43$ MPa), but far away from the parallel deformation value ($E = 18$ MPa). The contribution to the smectic layering deformation for the polydomain deformation in absolute values is $E_{pre} = 0.52$ MPa, which lays between the values for the parallel ($E_{pre} = 11.0$ MPa) and perpendicular ($E_{pre} = 0.33$ MPa) deformations of the monodomain. That means that less energy is required to deform a random distribution of domains than to shear mesogens between smectic layers, but the order of magnitude is comparable with the energetic level of destroying a monodomain. The large nonreversible deformations (up to $\lambda \approx 4.5$ for the polydomain and $\lambda \approx 9$ for the perpendicular monodomain deformation) indicate rearrangement of the structure, which can also be deduced from the low values of the corresponding slopes of $d\sigma_t/d\lambda = 0.27$ MPa ($1.5 < \lambda < 2.4$) and $d\sigma_t/d\lambda = 0.15$ MPa ($2.30 < \lambda < 6.00$), respectively (see Supporting Information, Figure SI-1).

Uniaxial stress–strain of the polydomain sample revealed three different strain regions differentiated by the slope

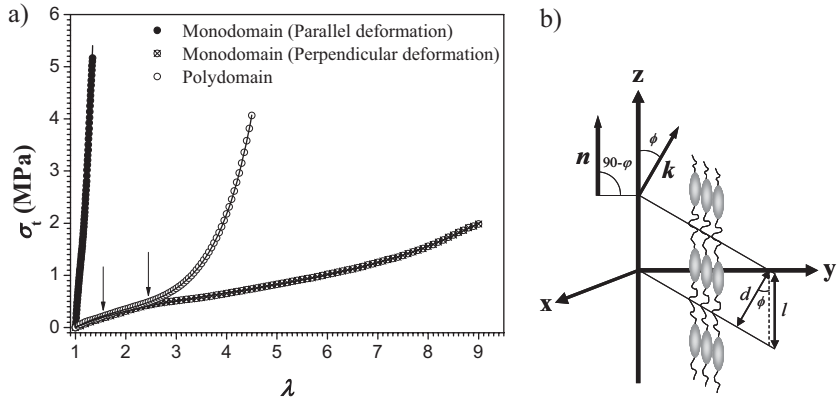

Figure 1. a) Uniaxial true stress-strain (σ_t vs. λ) curves of a monodomain sample parallel (●) and perpendicular (⊗) to the director, and of a polydomain sample (○) of the corresponding SmC MCLCE at 25 °C. The arrows indicate regions of changing slope; refer to text. The solid curves are the fits to the data points. b) Structure of a SmC MCLCE. The distances of the layers (*d*), length (*l*) between repeating units, and angles of monomers (90-φ) and layers (ϕ) with respect to the stretching direction **z** are shown.

Table 1. Fitting parameters (a, b, c, d, f), the Young's modulus (E) and its components (E_{lin}, E_{exp}, E_{pre}) for all three uniaxial stress–strain experiments.

Sample	a	b	c	d	f	E	E_{lin}	E_{exp}	E_{pre}
	MPa	kPa		kPa		MPa	MPa	MPa	MPa
Monodomain (parallel)	–	1580	4.3	350	31	17.8	–	6.8	11.0
Monodomain (perpendicular)	0.09	27.7	0.44	336	0.97	0.43	0.09	0.01	0.33
Polydomain	–	27.9	1.4	336	1.5	0.56	–	0.04	0.52

of the true stress–strain curve: (I) from $\lambda = 1.0$ to 1.5, (II) from $\lambda = 1.6$ to 2.4 and (III) from 2.5 $\lambda =$ to 4.5, which might indicate different deformation mechanisms with respect to the uniaxial stress–strain deformation parallel or perpendicular to the director on monodomain samples with conical layer distribution. The slope value ($d\sigma_t/d\lambda$) in this curve and the initial pre-stress component (E_{pre}) of the Young's modulus (E) are lower than the uniaxial stress–strain parallel to the director of the monodomain sample, and resembles the stress–strain behaviour of the uniaxial stress–strain perpendicular to the director of the monodomain sample but with a rising of the stress at lower strain values. Thus, the three regions seen during the deformation of the polydomain sample can be explained by the breaking of the random distribution of the domains, the reorientation of those domains, and the stretching of the polymer backbones (Figure 1a).

Several previous communications have reported the soft plateau region[5,12,13] and necking[10,11] during PM transformations, but have only used the mechanical response from the nominal stress ($\sigma_n = F/A_0$) in non-equilibrium conditions. The present results use true stress ($\sigma_t = \sigma_n \cdot \lambda$) versus strain ($\lambda$), and are thus closer to reality and to the existent theories.

Polydomain–Monodomain Structure Transformation

As observed from the uniaxial stress–strain experiments, the mechanical properties of this elastomer strongly depend on the direction of the applied force and the initial orientational state of the mesogens. X-ray experiments were performed on the polydomain sample under uniaxial deformation in order to elucidate structural changes of the smectic layering and the mesogens orientation in the elastomer in the three strain regions, and to compare these changes to the previous deformations when the elastomer has a conical distribution of the smectic layers.

In Figure 2, the X-ray pictures of the nonstretched sample ($\lambda = 1.0$) at 25 °C are shown, and of the sample stretched at different strain values of $\lambda = 1.5$, 1.6, 2.4, 2.5 and 4.5. Additionally, the WAXS and SAXS azimuthal intensity distributions are given. The nonstretched sample exhibits a random distribution in the small-angle and in the wide-angle region, indicating the presence of a polydomain with respect to the mesogens and smectic layers in both cases. Upon stretching the sample, the small-angle and wide-angle azimuthal distributions are no longer isotropic, showing that the deformation process goes to a monodomain formation with the conical distribution of smectic layers.

Starting from the nonstretched structure, spontaneous and continuous layer redistribution is observed toward a uniform orientation of the layer normal in the plane perpendicular to the applied stress (Figure 3a). The mechanical field is seen to couple to the smectic layers, and forces the orientation of both mesogens and layers to a conical layer distribution structure.

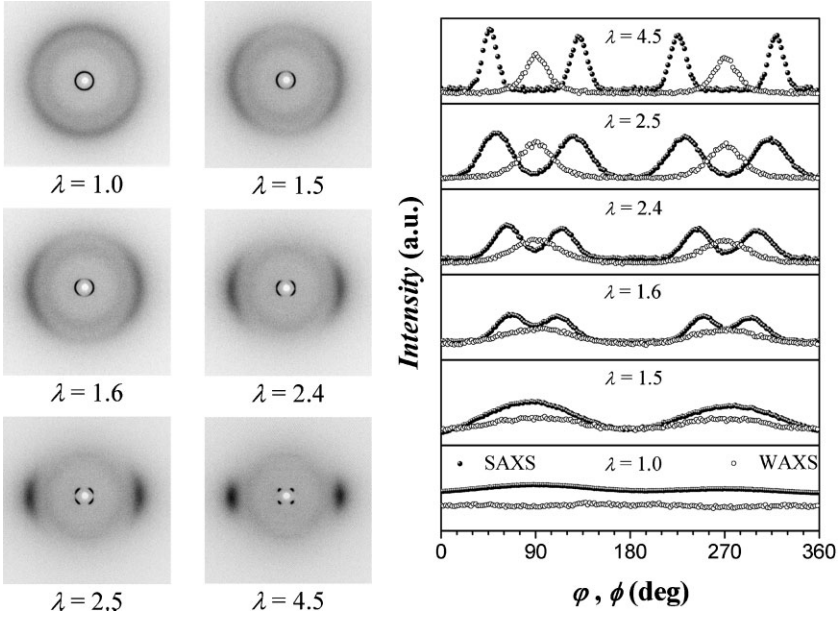

Figure 2. X-ray pictures of the SmC MCLCE at 25 °C, and its WAXS and SAXS azimuthal intensity distributions at the uniaxial strain of $\lambda = 1.0$, 1.5, 1.6, 2.4, 2.5 and 4.5. (Experiments at all different strain values are available in the Supporting Information, Figure SI-7.)

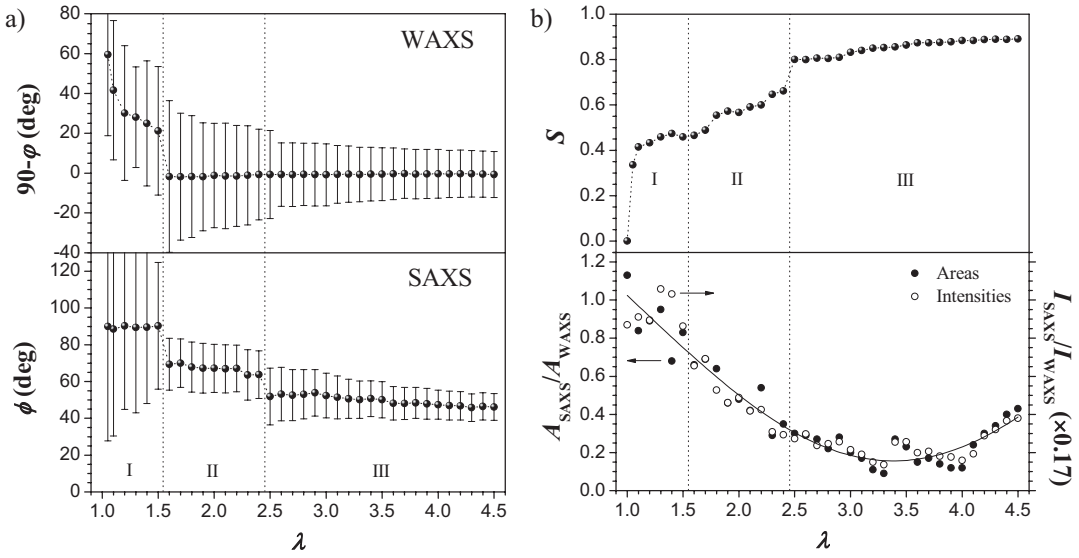

Figure 3. a) Peak maxima in the WAXS (90-φ) and SAXS (ϕ) azimuthal intensity distributions as a function of uniaxial strain, λ. b) Order parameter S, area ratio and intensity ratio between the SAXS and WAXS peak maxima as function of uniaxial strain, λ.

In the strain regime of $1.0 \leq \lambda \leq 1.5$ (Figure 1a), the polydomain sample assumes a weakly ordered conical mesogen distribution which resembles a SmC_A phase (see Supporting Information, Figure SI-4), where the layer normal is around $\phi = 90^\circ$ (two broad azimuthal maxima) and the mesogens show an average strain dependent angle of 90-$\varphi = 60$–20° (four broad azimuthal maxima). This SmC_A distribution of layers has the layer normal perpendicular to the applied mechanical field and looks like the slow motion deformation process already observed during the deformation of main-chain liquid-crystalline polymers.[40] The first steps during the orientational process are actually identified by the strong increase of the order parameter from $S = 0.00$ at $\lambda = 1.0$ to $S = 0.46$ at $\lambda = 1.5$ (Figure 3b), where S reflects the product of the orientational and director order parameter.

In the strain regime of $1.6 \leq \lambda \leq 2.4$, where the stress–strain curve is almost linear (Figure 1a), the previous SmC_A elastomer becomes SmC with an enhancement of the order of both mesogens and layers. A huge layer rotation of the layer normal occurs by 38° from $\phi = 90^\circ$ to 52° (four azimuthal maxima) – with a slope down of 5° of difference in the middle part – and the mesogens are distributed around an angle of 90-$\varphi = 0^\circ$ (two azimuthal maxima). During this rotational process of the layers, the order parameter increases as function of the uniaxial strain from $S = 0.47$ to 0.66 gradually (Figure 3b), where this is an indication of ordering of the system.

Finally, in the strain regime of $2.5 \leq \lambda \leq 4.5$ (Figure 1a), all mesogens align to the stretching direction (90-$\varphi = 0^\circ$, with two azimuthal maxima) and the layers adopt the final conical distribution from $\phi = 52^\circ$ to 46° (four azimuthal maxima), similar to the final optimisation of the packing of the mesogenic monomer units under strain in the stretching process for a conical layer distribution system under uniaxial stress parallel to the director.[1] The slope at break ($d\sigma_t/d\lambda_{max} = 5.2$ MPa), however, does not recover the value observed for the deformation parallel to the director ($d\sigma_t/d\lambda_{max} = 30$ MPa), but it is one order of magnitude higher than for the deformation perpendicular to the director ($d\sigma_t/d\lambda_{max} = 0.53$ MPa). Furthermore, the intensity distribution of the wide-angle reflections narrows, indicating an increase of the order parameter from $S = 0.80$ to 0.89. After complete orientation, a tilt angle is observed that corresponds to the tilt angle of the monodomain sample under uniaxial strain parallel to the director. As mentioned in literature for SCLCEs[2,3] or MCLCEs,[5,13] a spontaneous rising of the order parameter at certain stress thresholds has been observed. Somehow, a minimum stress is required to induce the rearrangement of the mesogens in the range of 10 kPa. This can be explained for SCLCEs, where the coupling of the mesogens to the polymer backbone is not that efficient, but for MCLCEs any applied stress should immediately induce order because of the direct coupling between the polymer backbone and the mesogens. This was also our observation: a continuous increase of the order parameter was measured when pulling the sample. Thus, no linear elastic region is present and a continuous deformation appears along the experiment (see Supporting Information, Figure SI-5).

The analysis of the intensity distribution of the small-angle reflections reveals a correlation length of the smectic structure of about $\xi = 38 \pm 2$ nm (15 ± 1 layers),[1,41,42] which remains unchanged during the deformation process

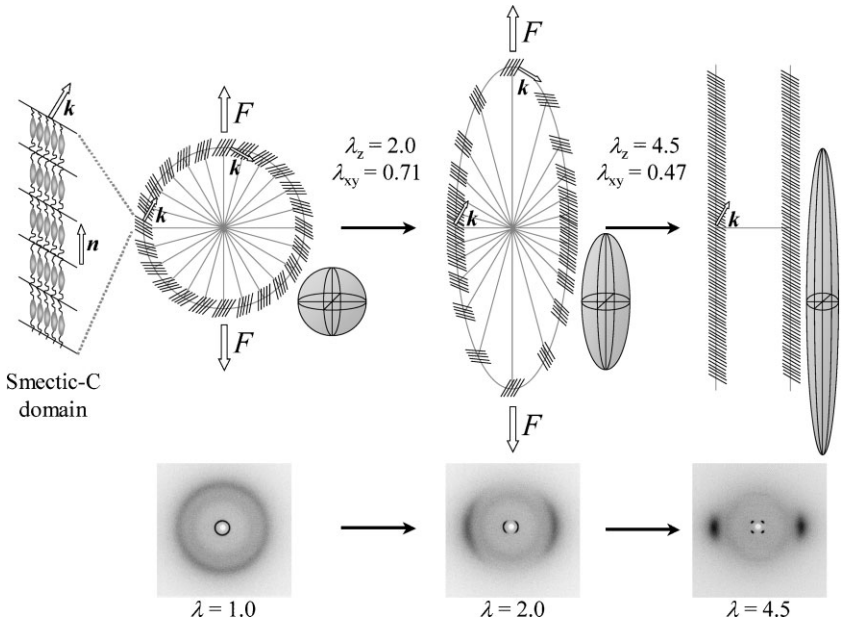

Figure 4. Polydomain–monodomain transformation process of a SmC MCLCE: from a spherical to a fully eccentric ellipsoidal distribution of domains. The figures are 2D representations of a 3D situation, and only the clockwise representation of the domains is shown here.

of the elastomer. The area ratio and intensity ratio between the small-angle and wide-angle reflections show the same tendency (Figure 3b). Both decrease during the polydomain–monodomain transformation, reaching a minimum at the strain value of $\lambda = 3.3$, and increasing again up to the breaking of the sample, as a sign of the rearrangement of the smectic layering.

The model for better understanding this transformational process is depicted in Figure 4. Starting from a random distribution of domains (spherical distribution) with several layers in a SmC fashion, the sample is stretched and the same domains are placed in a new location, where their scattering is no longer spherically distributed. The intermediate prolate ellipsoidal distribution of domains enhances the scattering of those domains where the mesogens are parallel to the stretching direction. The final conformation is a fully eccentric ellipsoid with only two possible layer distributions, as the monodomain sample.

Conclusion

The polydomain–monodomain orientational process of a SmC MCLCE under uniaxial stress–strain deformation has been compared to its corresponding conical layer distribution sample (monodomain). Stress–strain and X-ray experiments were performed to identify structural modifications during deformation. This orientational transformation has an intermediate stress–strain behaviour with respect to the mechanical response when a force is applied parallel or perpendicular to the director of a conical layer distribution structure of SmC MCLCE.

Three different strain regions have been identified during the deformation of the polydomain sample: (I) the breaking of the random distribution of the domains to a weakly ordered SmC_A mesophase ($E = 0.56$ MPa), (II) the reorientation of those domains to a preferred direction to reach an ordered SmC mesophase ($d\sigma_t/d\lambda = 0.27$ MPa) and (III) the stretching of the polymer backbones in the SmC mesophase ($d\sigma_t/d\lambda_{max} = 5.2$ MPa). Thus, the applied mechanical field couples to both the mesogens and the layers.

The process is explained by the deformation of a spherical distribution of domains after reaching a fully eccentric prolate ellipsoidal distribution. Thus, the random distribution of smectic layers (polydomain) becomes an anisotropic distribution of a conical layered structure (monodomain).

Acknowledgements: The authors acknowledge financial support from the *Research Training Networks* FUNCTIONAL LIQUID-CRYSTALLINE ELASTOMERS (FULCE-HPRNCT-2002-00169) and *Fonds der Chemischen Industrie*.

Received: September 12, 2010; Revised: October 2, 2010; Published online: December 14, 2010; DOI: 10.1002/marc.201000590

Keywords: liquid-crystalline elastomer; polydomain–monodomain transformation; smectic; stress–strain; X-ray

[1] A. Sánchez-Ferrer, H. Finkelmann, *Macromolecules* **2008**, *41*, 970.
[2] E. R. Zubarev, R. V. Talroze, T. I. Yuranova, N. A. Plate, H. Finkelmann, *Macromolecules* **1998**, *31*, 3566.
[3] S. M. Clarke, E. M. Terentjev, I. Kundler, H. Finkelmann, *Macromolecules* **1998**, *31*, 4862.
[4] C. Ortiz, C. K. Ober, E. J. Kramer, *Polymer* **1998**, *39*, 3713.
[5] C. Ortiz, M. Wagner, N. Bhargava, C. K. Ober, E. J. Kramer, *Macromolecules* **1998**, *31*, 8531.
[6] C. Ortiz, R. Kim, E. Rodighiero, C. K. Ober, E. J. Kramer, *Macromolecules* **1998**, *31*, 4074.
[7] M. Giamberini, V. Ambrogi, P. Cerruti, C. Carfagna, *Polymer* **2006**, *47*, 4490.
[8] I. A. Rousseau, P. T. Mather, *J. Am. Chem. Soc.* **2003**, *125*, 15300.
[9] H. P. Patil, J. Liao, R. C. Hedden, *Macromolecules* **2007**, *40*, 6206.
[10] H. P. Patil, D. M. Lentz, R. C. Hedden, *Macromolecules* **2009**, *42*, 3525.

[11] W. Ren, P. J. McMullan, A. C. Griffin, *Macromol. Chem. Phys.* **2008**, *209*, 1896.
[12] W. Ren, P. J. McMullan, A. C. Griffin, *Phys. Status Solidi B* **2009**, *246*, 2124.
[13] R. Ishige, K. Osada, H. Tagawa, H. Niwano, M. Tokita, J. Watanabe, *Macromolecules* **2008**, *41*, 7566.
[14] K. Hiraoka, W. Sagano, T. Nose, H. Finkelmann, *Macromolecules* **2005**, *38*, 7352.
[15] P. Heinze, H. Finkelmann, *Macromolecules* **2010**, *43*, 6655.
[16] P. Papadopoulos, P. Heinze, H. Finkelmann, F. Kremer, *Macromolecules* **2010**, *43*, 6666.
[17] S. V. Fridrikh, E. M. Terentjev, *Phys. Rev. E* **1999**, *60*, 1847.
[18] J. S. Biggins, M. Warner, K. Bhattacharya, *Phys. Rev. Lett.* **2009**, *103*, 037802.
[19] J. S. Biggins, K. Bhattacharya, *Phys. Rev. E* **2009**, *79*, 061705.
[20] T. C. Lubensky, E. M. Terentjev, M. Warner, *J. Phys. II Fance* **1994**, *4*, 1457.
[21] O. Stenull, T. C. Lubensky, *Phys. Rev. Lett.* **2005**, *94*, 018304.
[22] J. M. Adams, M. Warner, *Phys. Rev. E* **2005**, *72*, 011703.
[23] J. M. Adams, M. Warner, *Phys. Rev. E* **2006**, *73*, 031706.
[24] O. Stenull, T. C. Lubensky, *Phys. Rev. E* **2007**, *75*, 031711.
[25] J. Weilepp, H. R. Brand, *Macromol. Theory Simul.* **1998**, *7*, 91.
[26] J. M. Adams, M. Warner, *Phys. Rev. E* **2005**, *71*, 021708.
[27] O. Stenull, T. C. Lubensky, *Phys. Rev. E* **2007**, *76*, 011706.
[28] J. M. Adams, M. Warner, O. Stenull, T. C. Lubensky, *Phys. Rev. E* **2008**, *78*, 011703.
[29] O. Stenull, T. C. Lubensky, *Phys. Rev. E* **2006**, *73*, 030701.
[30] O. Stenull, T. C. Lubensky, *Phys. Rev. E* **2006**, *74*, 051709.
[31] J. M. Adams, M. Warner, *Phys. Rev. E* **2008**, *77*, 021702.
[32] R. Lovell, G. R. Mitchell, *Acta Crystallogr. A* **1981**, *37*, 135.
[33] G. R. Mitchell, A. H. Windle, *Development in Crystalline Polymers-2*, D. C. Basset, Ed., Elsevier Applied Science, London 1988; Vol. 3, p. 115.
[34] A. Sánchez-Ferrer, H. Finkelmann, *Mol. Cryst. Liq. Cryst.* **2009**, *508*, 348.
[35] A. Sánchez-Ferrer, H. Finkelmann, *Mol. Cryst. Liq. Cryst.* **2009**, *508*, 357.
[36] S. Krause, R. Dersch, J. H. Wendorff, H. Finkelmann, *Macromol. Rapid Commun.* **2007**, *28*, 2062.
[37] E. Nishikawa, H. Finkelmann, H. R. Brand, *Macromol. Rapid Commun.* **1997**, *18*, 65.
[38] N. Aßfalg, H. Finkelmann, *Macromol. Chem. Phys.* **2001**, *202*, 794.
[39] M. Warner, E. M. Terentjev, *Liquid Crystal Elastomers*, Oxford University Press, USA 2007, p. 310.
[40] K. Osada, M. Koike, H. Tagawa, S. Hunaoka, M. Tokita, J. Watanabe, *Macromolecules* **2005**, *38*, 7337.
[41] A. S. Muresan, B. I. Ostrovskii, A. Sáchez-Ferrer, H. Finkelmann, W. H. de Jeu, *Eur. Phys. J. E* **2006**, *19*, 385.
[42] W. H. de Jeu, E. P. Obraztsov, B. I. Ostrovskii, W. Ren, P. J. McMullan, A. C. Griffin, A. Sánchez-Ferrer, H. Finkelmann, *Eur. Phys. J. E* **2007**, *24*, 399.